TRANSIENT ANALYTICAL SOLUTION OF TEMPERATURE DISTRIBUTION AND FRACTURE LIMITS IN PULSED SOLID-STATE LASER ROD

by

Khalid S. SHIBIB, Mohammed A. MUNSHID, Mohammed Jalal ABDUL RAYYAK, and Luma Hasan SALMAN*

Laser and Optoelectronics Engineering Department, University of Technology, Baghdad, Iraq

Original scientific paper
https://doi.org/10.2298/TSCI141011090S

The exact analytical solution of axis-symmetry transient temperature and Tresca failure stress in pulsed mode solid-state laser rod is derived using integral transform method. The result obtained from this work is compared with previously published data and good agreement is found. The effect of increasing period is studied, and it is found that at constant pulse width as the period is increased, the allowable pumping power is increased too. Furthermore, the effect of changing pulse width with a constant period is studied, and it is found that as the pulse width is increased, the allowable pumping power is decreased. The effect of duty cycle is studied also and it is found that as duty cycle is increased the allowable pumping power is decreased. This work permits proper selection of pulse width, period and duty cycle to avoid laser rod fracture while obtaining maximum output laser power in the designing of laser system.

Key words: *pulsed solid-state rod, heat, Tresca failure stress, integral transform method*

Introduction

The main factor that limits the power scaling of diode-end-pumped solid-state lasers is the heat induced inside gain medium. The generated heat inside the laser gain medium causes steep temperature gradients inside the crystal which produce stress that may lead to fracture [1]. Fracture occurs when the thermally induced stress exceeds the ultimate strength of the material. The temperature gradient in the gain medium causes laser beam distortion due to thermal lensing, depolarization loss due to stress induced birefringence and ultimately fracture of the laser rod [2]. Stresses inside the laser rod are induced due to the hotter inner region of the rod that is restricted from expansion by the cooler outer region [3]. Moreover when the induced stresses in the laser rod exceed the tensile strength of the material, the rod will fracture and cause the pump and laser beams to be heavily distorted. The severe distortion losses might even cause the laser to no longer operate. Crystal fracture is one of the primary limiting factors in the power scaling of diode-end-pumped solid-state lasers which makes it an important effect that has to be considered in the design process [1].

* Corresponding author; e-mail: luma_laser@yahoo.com

One of the most popular method of scaling output laser power is by using pulsed mode where high out energy can be obtained in short time.

Many works devoted to determine temperature distribution and induced stress in laser rod. Robinson [4] determined the thermal transient effects in laser rods, such as the temperature distribution and the effect of rod distortion on a collimated light beam passing through the rod. Huang *et al.* [5] solved 3-D heat conduction models under the cylindrical co-ordinate using the base of pumped structure of face-pumped disk laser. The transient solution of temperature field distribution and thermal stress distribution was got through integral transform method. Bernhardi *et al*. [6] presented a 1-D time-dependent analytical thermal model of the temperature and the corresponding induced thermal stresses on the pump face of quasi– continuous wave (CW) diode-end-pumped Tm:YLF laser rods also a numerical solution for this problem was used. Liu *et al.* [7] solved analytically the transient heat conduction and thermal effects in pulse end-pumped fiber laser. For the arbitrary temporal shape of pump pulse, a 3-D temperature expression was derived via an integral transform method, and the thermal stress field was deduced through solving the Navier displacement equations. Shibib *et al*. [8, 9] derived the transient analytical solutions of temperature distribution, stress, strain, and optical path difference in convectional cooled (CW) end-pumped laser rod. The results were compared with other works and good agreements were found.

In this work, an axis-symmetry equation for temperature distribution and Tresca failure stress through pulsed end-pumped laser rod is derived using integral transform method where the fracture limits in pulsed solid-state laser rod is obtained also the effects of duty cycle on temperature distribution and fracture limit are studied. The result obtained using the derived equation is compared with other published work and good agreement is obtained.

Theory

The solution of heat equation in laser rod permits the prediction of the temperature distribution so as to determine the thermal effects in the laser rod. The transient temperature distribution through the laser rod can be determined by solving the axis-symmetry heat equation.

The derivation of axis-symmetry heat equation is obtained from [10, 11]. A major objective in a conduction analysis is to determine the temperature field in a medium that resulting from conditions imposed inside and on rod boundaries. Assume symmetrical boundary conditions about circumferential direction and constant thermal properties of laser crystal then heat equation can be written:

$$\frac{\partial^2 T}{\partial r^2}+\frac{1}{r}\frac{\partial T}{\partial r}+\frac{\partial^2 T}{\partial z^2}+\frac{q}{k}=\frac{\rho c_p}{k}\frac{\partial T}{\partial t} \tag{1}$$

Refer to fig. 1 which shows the laser rod and cooling arrangements together with pumping location, the boundary conditions can be written:

$$k\left.\frac{\partial T}{\partial r}\right|_{r=r_o}=h_e(T_\infty-T) \quad \text{at} \quad r=r_\text{o} \tag{2}$$

$$k\left.\frac{\partial T}{\partial z}\right|_{z=0}=h_a(T_\infty-T) \quad \text{at} \quad z=0 \tag{3}$$

$$-k\left.\frac{\partial T}{\partial z}\right|_{z=l} = h_a(T_\infty - T) \quad \text{at} \quad z = l \tag{4}$$

$$\frac{\partial T}{\partial r} = 0 \quad \text{at} \quad r = 0 \tag{5}$$

Convection boundary conditions are assumed at the facets of the rod, fig. 1. The initial and environmental temperatures, T_∞, are assumed to be 25 °C. The laser rod is mounted in Cu heat sink. Heat conductivity is provided by an indium layer between the Cu and the crystal. An adjustable water flow rate can be implemented to give the required edge heat transfer coefficient. The part of absorbed power that converts to heat act as heat generation inside a laser crystal. For pumping power that has a top hat beam distribution, heat generation inside laser rod can be written [3, 12]:

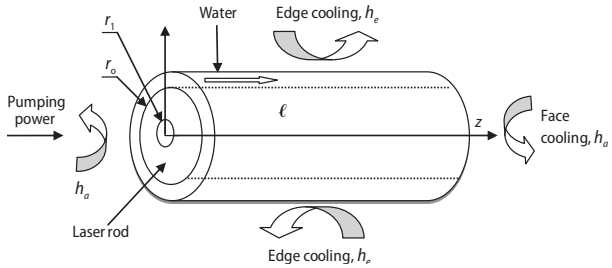

Figure 1. Laser rod and its boundary conditions

$$q = \begin{cases} \dfrac{\alpha\, H_f\, P_{ab} \exp(-\alpha z)}{\pi r_1^2} & 0 \le r \le r_1,\ t \ge 0 \\ 0 & r_1 \le r \le r_o,\ t \ge 0 \\ 0 & t < 0 \end{cases} \tag{6}$$

With the previous equation that modeled the heat generation inside the laser rod, the conduction heat equation for a solid cylinder of radius, r_o, and length, ℓ, with boundary conditions described in eqs. (2)-(5) can be solved through integral transform method [13]:

$$\theta(r,z,t) = T - T_\infty = \sum_{m=1}^{\infty}\sum_{p=1}^{\infty} \frac{R_o(\beta_m, r) Z(\eta_p, z)}{N(\beta_m) N(\eta_p)} \exp\left[-\frac{k}{\rho c_p}(\beta_m^2 + \eta_p^2)t\right] \cdot$$
$$\cdot \left[\frac{1}{\rho c_p} \int_{t'=0}^{t} \exp\left[\frac{k}{\rho c_p}(\beta_m^2 + \eta_p^2)t'\right] \bar{\bar{g}}(\beta_m, \eta_p, t')\mathrm{d}t'\right] \tag{7}$$

where

$$\bar{\bar{g}}(\beta_m, \eta_p, t') = \int_{z'=0}^{\ell} \int_{r'=0}^{r1} \delta(t) r' R_o(\beta_m, r') Z(\eta_p, z') g(t') \mathrm{d}r' \mathrm{d}z' \tag{8}$$

Here $\bar{\bar{g}}(\beta_m, \eta_p, t')$ is the laser pulse shape, also eigenfunction $R_o(\beta_m, r)$ of differential equation is obtained from Ozisik [13]:

$$R_o(\beta_m, r) = J_o(\beta_m r) \tag{9}$$

and the Norms $N(\beta_m)$ of the differential equation are [13]:

$$\frac{1}{N(\beta_m)} = \frac{1}{N_m} = \frac{2k^2\beta_m^2}{r_o^2 J_o(\beta_m r_o)(h_e^{\,2} + k^2\beta_m^2)} \tag{10}$$

Using convection boundary conditions, then the eigenvalues, β_m, of differential equation are the positive roots of the next equation [13]:

$$h_e J_o(\beta_m r_o) - k\beta_m J_1(\beta_m r_o) = 0 \tag{11}$$

Newton-Raphson method is used to obtain the successive values of the roots (*i. e.* β_m where m is varying from 1 to infinity). For convection boundary conditions at the facets of the rod, assuming equal convection heat transfer coefficients at both end of the rod, then eigenfunction $Z(\eta_p, z)$ of differential equation can be obtained [13]:

$$Z(\eta_p, z) = \eta_p \cos(\eta_p z) + H\sin(\eta_p z) \tag{12}$$

Here $H = h_a/k$ where h_a is the convection heat transfer coefficient from rod facets and for naturally cooled rod facets, it is equal to 27.5 W/m^{2}K [14].

Then the Norms, $N(\eta_p)$, of differential equation can be written:

$$\frac{1}{N(\eta_p)} = \frac{1}{N_p} = \frac{2}{\left(\eta_p^2 + H^2\right)\left(l + \dfrac{H}{\eta_p^2 + H^2}\right) + H} = \frac{2}{l\left(\eta_p^2 + H^2\right) + 2H} \tag{13}$$

Then eigenvalues, η_p, of differential equation are the positive roots of next equation [13]:

$$\tan(\eta_p l) = \frac{2\eta_p H}{\eta_p^2 - H^2} \tag{14}$$

Again Newton-Raphson method is used to obtain the successive values of the roots, and the main equation of the solution can be written:

$$\theta = T - T_\infty = \sum_{m=1}^{\infty}\sum_{p=1}^{\infty} \frac{J_o(\beta_m r)[\eta_p \cos(\eta_p z) + H\sin(\eta_p z)]}{N_m N_p} \cdot$$
$$\cdot \exp\left[-\frac{k}{\rho c_p}\left(\beta_m^2 + \eta_p^2\right)t\right]\left[\frac{1}{\rho c_p}\int_{\tau=0}^{\tau} \exp\left[\frac{k}{\rho c_p}\left(\beta_m^2 + \eta_p^2\right)\tau\right] g(\tau)\,\mathrm{d}\tau\right] \tag{15}$$

where τ is the time of pumping. For top hat beam distribution the function $g(\tau)$ can be written:

$$g(\tau) = \int_0^{\ell}\int_0^{r_1} \delta(t)\frac{\alpha H_f P_{ab}}{\pi r_1^2} J_o(\beta_m r)\exp(-\alpha z)\left[\eta_p \cos(\eta_p z) + H\sin(\eta_p z)\right] r\,\mathrm{d}r\,\mathrm{d}z \tag{16}$$

Assuming pulse mode where pulse laser temporal shape is assumed as square incident laser irradiance, then $\delta(t)$ is equal to one when pulse is on and zero if pulse is off. The integration in z co-ordinate can be solved directly:

$$\int_0^t \exp(-\alpha z)[\eta_p \cos(\eta_p z) + H \sin(\eta_p z)]\,\mathrm{d}z = \frac{\eta_p}{\alpha^2 + \eta_p^2}\{\exp(-\alpha l)[\eta_p \sin(\eta_p l) - \alpha \cos(\eta_p l) + \alpha]\} +$$
$$+\frac{H}{\alpha^2 + \eta_p^2}\{\exp(-\alpha l)[-\alpha \sin(\eta_p l)] - \eta_p \cos(\eta_p l) + \eta_p\} = A_p \tag{17}$$

Also, the integration in r co-ordinate can be solved directly:

$$\int_0^{r_1} J_o(\beta_m r)\, r\,\mathrm{d}r = \frac{r_1 J_1(\beta_m r_1)}{\beta_m} \tag{18}$$

Combining the results of integrations of eqs. (17) and (18) into eq. (16) and when pulse is on $\delta(t) = 1$, the function $g(\tau)$ can be written:

$$g(\tau) = A_p \frac{\alpha H_f P_{ab} J_1(\beta_m r_1)}{\pi r_1\, \beta_m} \tag{19}$$

Finally, one can obtain the transient temperature distribution through pulsed end--pumped laser rod that cooled from its edge and facets by substituting eq. (19) into eq. (15) and carrying time integration then:

$$\theta(r,z,t) = T - T_\infty = \frac{\alpha H_f P_{ab}}{\pi k r_1} \sum_{m=1}^{\infty}\sum_{p=1}^{\infty} A_p \frac{J_o(\beta_m r) J_1(\beta_m r_1)[\eta_p \cos(\eta_p z) + H \sin(\eta_p z)]}{(\beta_m^2 + \eta_p^2) N_m N_p \beta_m} \cdot$$
$$\cdot \exp\left[-\frac{k}{\rho c_p}(\beta_m^2 + \eta_p^2)t\right] \times \left\{\exp\left[\frac{k}{\rho c_p}(\beta_m^2 + \eta_p^2)t_o\right] - 1\right\} \sum_{n=1}^{N} \exp\left[(n-1)\frac{k}{\rho c_p}(\beta_m^2 + \eta_p^2)T_o\right] \tag{20}$$

This equation represents the transient temperature distribution through pulsed end − pumped laser rod that cooled from its edge and facets. Note that fifteen roots are sufficient to predict the precise value of the temperatures. Transient solution can be also obtained starting from rest. From the previous solution, the temperature history in laser rod can be obtained until either a quasi steady-state or failure stress is reached.

Tresca failure stress equation

As the laser rod heated due to the part of the absorbed power that converts to heat, there will be a temperature steep which will induce thermal stresses. Since the laser rod is symmetric, the thermal stress distribution can be obtained depending on heat flexibility theory, stress balance equation, geometry equation, and generalized Hooke equation of stress distortion [15]:

$$\sigma_{rr} = \frac{\gamma E}{1-\nu}\left[\frac{1}{r_o^2}\int_0^{r_0} \theta(r,z,t) r\,\mathrm{d}r - \frac{1}{r^2}\int_0^{r} \theta(r,z,t) r\,\mathrm{d}r]\right] \tag{21}$$

$$\sigma_{\theta\theta} = \frac{\gamma E}{1-\nu}\left[\frac{1}{r_o^2}\int_0^{r_0} \theta(r,z,t) r\,\mathrm{d}r + \frac{1}{r^2}\int_0^{r} \theta(r,z,t) r\,\mathrm{d}r - \theta(r,z,t)\right] \tag{22}$$

$$\sigma_{zz} = \frac{2\gamma E}{1-\nu}\left[\frac{1}{r_o^2}\int_0^{r_0}\theta(r,z,t)r\mathrm{d}r - \theta(r,z,t)\right] \tag{23}$$

Using a plane-strain approximation and assuming that the stress in the axial direction is zero, we may calculate the radial and tangential stresses from the temperature profile and using the Tresca failure formula.

Here is:

$$J_2(x) = \frac{2J_1(x)}{x} - J_o(x) \tag{24}$$

Assuming $z = 0$ then Tresca failure could be written [9, 16]:

$$\sigma_T = \left|\sigma_{\theta\theta} - \sigma_{rr}\right| = \frac{\gamma E}{1-\nu}\left|\frac{2}{r}\int_0^{r}\theta(r,0,t)r\mathrm{d}r - \theta(r,0,t)\right| \tag{25}$$

Incorporating the equation of θ and carrying the integration result in:

$$\sigma_T = \left|\sigma_{\theta\theta} - \sigma_{rr}\right| = \frac{\gamma E\alpha H_f P_{ab}}{(1-\upsilon)\pi k r_1}\sum_{m=1}^{\infty}\sum_{p=1}^{\infty}A_p\frac{J_1(\beta_m r_1)J_2(\beta_m r)\eta_p}{\beta_m N_p N_m(\beta_m^2+\eta_p^2)}\times\exp\left[-\frac{k}{\rho c_p}(\beta_m^2+\eta_p^2)t\right]\cdot$$
$$\cdot\left\{\exp\left[\frac{k}{\rho c_p}(\beta_m^2+\eta_p^2)t_o\right]-1\right\}\sum_{n=1}^{N}\exp\left[(n-1)\frac{k}{\rho c_p}(\beta_m^2+\eta_p^2)T_o\right] \tag{26}$$

Which represent the Tresca failure stress (*i. e.* stress at which failure occurs).

Results and discussion

A computer program was written to obtain the successive roots for β_m, η_p using Newton- Raphson method with proper starting initial guess roots, summing the result successively to obtain the temperature distribution and Tresca failure stress at each time step. To validate our analytical solution, a comparison is made between the result of this work and that obtained by Bernhardi *et al.* [6] using the same parameters mention in tab. 1. Facets cooling is assumed in this work. To match the assumed insulated facets in the work of Bernhardi *et al.* [6], the value of the heat transfer coefficient is reduced much lower than that of the naturally cooled facets (*i. e.* $h_a \ll 27.5$ W/m^{2}K). A good nearby results is obtained for temperature and Tresca failure stress as shown in figs. 2 and 3 which verified the analytical solution derived in this work and the written program.

Table 1. Parameter values of the pumped Tm:YLF rod that implemented in the simulations

Parameter	Thermal model
Rod length, l	12 mm
Pump beam radius, r_1	0.47 mm
Rod radius, r_o	1.5 mm
Absorption coefficient, α	1.43 cm^{-1}
Thermal conductivity, k	7.2 (a-axis), 5.8 (c-axis) W/mK
Linear expansion coefficient, γ	13 (a-axis), 8.0 (c-axis) [10^{-6} K^{-1}]
Fractional heat load, H_f	0.33
Poisson's ratio, υ	0.33
Young's modulus, E	75 GPa
Density, ρ	3.9 g/cm^3
Specific heat capacity, c_p	0.79 J/gK
Lateral convection heat transfer coefficient, h_e	9000 W/m^{2}K
Face convection heat transfer coefficient, h_a	$\ll$27.5 W/m^{2}K

In this work the influence of increasing pulse width at constant period on maximum temperature distribution and Tresca failure stress in laser rod is studied. The result from derived equation of this work shows that at constant period as the

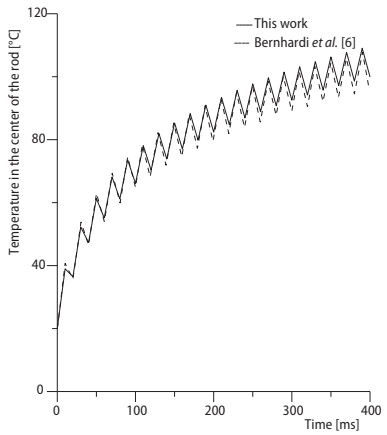

Figure 2. Comparison the result of this work with that obtained by Bernhardi *et al.* [6] for the parameters mentioned in tab. 1 for maximum temperature at the center of the Tm:YLF rod with pumping power 90 W, t_o = 10 ms, and T_o = 20 ms

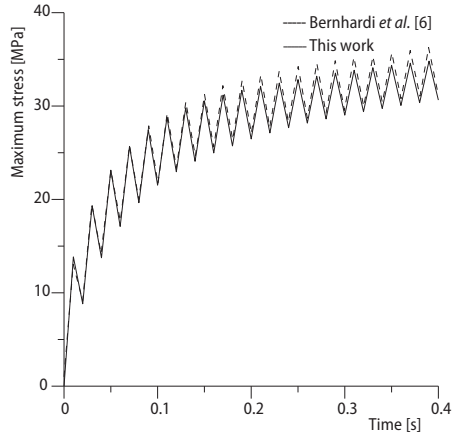

Figure 3. Comparison the result of this work with that obtained by Bernhardi *et al.* [6] for the parameters mentioned in tab. 1 for maximum Tresca failure stress that occurred in the Tm:YLF rod with pumping power 90 W, t_o = 10 ms, and T_o = 20 ms

pulse width is increased the maximum temperature that could be reached in the rod and the subsequent Tresca failure stress is increased too as shown in figs. 4 and 5.

The increase in the pulse period at constant pulse width permits more heat to flow out of laser rod before the subsequent pulse is induced so temperature will not be elevated as was happening at less period, fig. 6. This permits more pumping power before the fracture could happen, fig.7. It shows that at constant pulse width of 15 ms, the pulse period is varied from 20 ms to 400 ms to obtain its effect on the maximum allowable pumping power before fracture could happen. It is observed that as the period is increased with constant pulse width, the allowable pumping power that could cause failure is increased. This is due to increase in the cooling

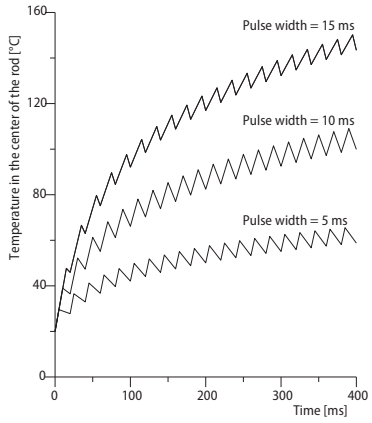

Figure 4. The influence of increasing pulse width at constant period of 20 ms on maximum temperature in the laser rod for parameter mentioned in tab. 1

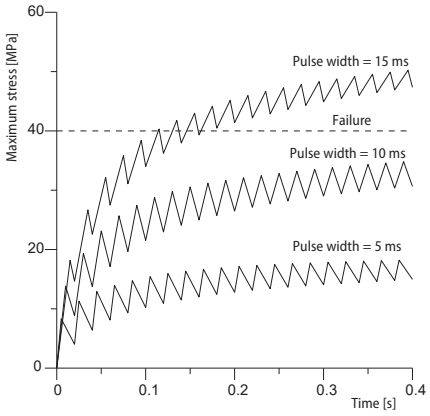

Figure 5. The influence of increasing pulse width at constant period of 20 ms on maximum Tresca failure stress in laser rod for parameter mentioned in tab. 1

time such that the rod temperature will be reduced which will also reduce the resulting stress as shown in fig. 7. This situation is limited where the cooling will no longer affect the scaling up in the power required to achieve failure. This situation occurs at period equal or greater than 400 ms where quasi steady-state was reached as shown in figs. 6 and 7.

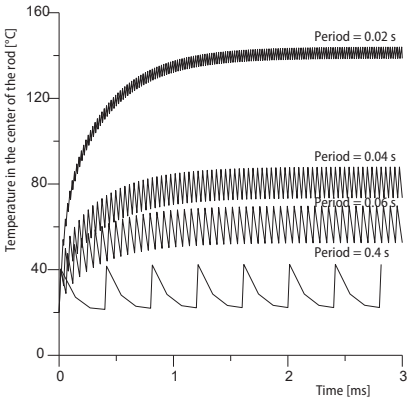

Figure 6. Effect of increasing period on pumping power that causes failure in laser rod at t_o = 15 ms and pumping power = 65.8 W for parameter mentioned in tab. 1

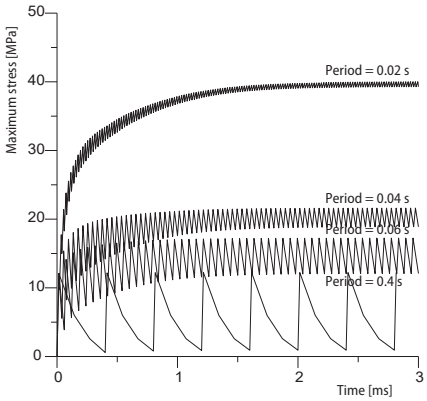

Figure 7. Effect of increasing period on pumping power that causes failure in laser rod at t_o = 15 ms and pumping power = 65.8 W for parameter mentioned in tab. 1

Table 2. Summarized values of maximum temperature, pumping power, and energy/pulse for different periods at constant pulse width of 10 ms with failure stress of 40 MPa

Pulse period, [ms]	50	100	400
Maximum temperature, [°C]	135.4	114.3	86.1
Pumping power, [W]	195.8	253.5	283

The results obtained from the derived equation of this work shown in tab. 2. It shows the maximum temperature and allowable pumping power at period of 50, 100, and 400 ms, respectively, for constant pulse width of 10 ms. It is clear that as period is increased the maximum temperature is decreased. This is due to the increase in cooling time before the subsequent pulse is induced so high allowable pumping power is expected, this situation is limited till quasi steady-state is reached.

The pumping power that may cause failure has been tested for different pulse widths and periods. Four pulse widths have been tested where their values are changed from 5 to 20 ms with different periods. The result are shown in fig. 8 which shows the allowable pumping power (that could cause failure) at different periods and pulse widths. It can be seen that as the pulse width is increased for the same period, the allowable pumping power that could cause failure is decreased. This is explainable since the time of inducing heat is increased which increase the temperature, temperature steep, and the subsequent induced thermal stress that could be induced in the rod.

The results obtained in tab. 3 show the influence of increasing pulse width for the same period on temperature distribution in laser rod. It is clear that as the pulse width is increased the maximum temperature is increased too. This is due to increase in the pumping time meanwhile the cooling time at off pumping is decreased which result in increasing in the tem-

Table 3. Summarized values of maximum temperature, pumping power for different pulse widths at constant periods of 400 ms with failure stress of 40 MPa

Pulse width, [ms]	5	10	15	20
Maximum temperature, [°C]	76	86.1	93.6	98.1
Pumping power, [W]	470	283	215.5	178

perature distribution and the maximum temperature that could occur in the rod which would decrease the allowable pumping power.

To achieve higher output power from a diode-end-pumped solid-state laser, a quasi-cw pump source is used with its advantage; the average thermal load is reduced through a reduced duty cycle. The quasi-cw pulsing leads to higher peak pump power, resulting in much higher laser output power during the quasi-cw pump pulse [6].

Figure 9 shows the allowable pumping power *vs.* duty cycle (the percentage of one period in which a signal is active) for different pulse widths obtained from the derived equation of this work from which one can observe that as duty cycle is increased the allowable pumping power is decreased. This is explainable since the cooling time after pumping is switched off is decreased which permits more heat to be stored in the rod resulting in an increase in the maximum temperature, temperature distribution, steep temperature which induce high thermal stress thus decreasing the allowable pumping power. For duty cycle less than 50% an increase in the allowable pumping power is observed as pulse width is decreased. This fact can be explained by knowing that more cooling is achieved since more time is allowed to cool the laser rod which results in less temperature gradient and subsequently less thermal stress.

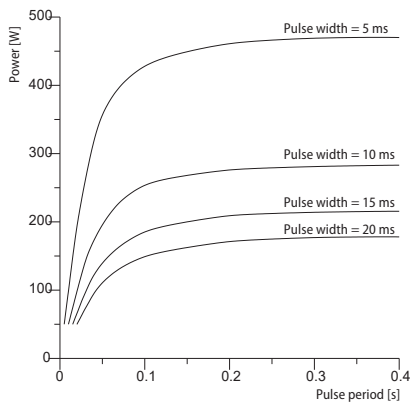

Figure 8. Effect of increasing period and pulse width on pumping power that causes failure in laser rod for parameter mentioned in tab. 1

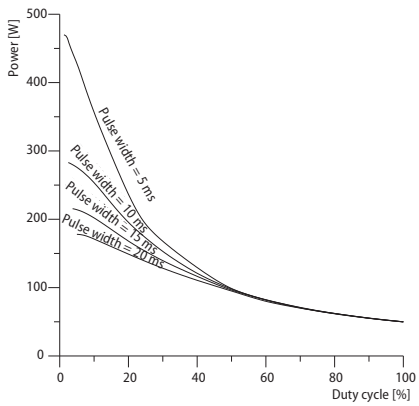

Figure 9. Effect of duty cycle on the allowable pumping power before fracture could happen in laser rod for parameter mentioned in tab. 1

Conclusions

The axis-symmetry transient analytical solution for temperature, stress, and Tresca failure stress in pulsed pumping laser rod is derived. The fracture limit that could be reached at different pumping power could be obtained using Tresca failure formula.

The results are compared with previously published work and good agreement is found. The effect of increasing period is studied, and it is found that as the period increased while pulse width remains constant the allowable pumping power is increased. The effect of changing pulse width with a constant period is studied, and it is found that as the pulse width is increased the allowable pumping power is decreased. The combined effect of pulse width and period is presented in duty cycle. It is observed that as duty cycle is increased the allowable pumping power is decreased. For duty cycle less than 50% an increase in the allowable pumping power is observed as pulse width is decreased since more time is allowed to cool the laser rod which results in less temperature gradient and subsequently less thermal stress.

Nomenclatures

c_p – specific heat, [Jkg^{-1}K^{-1}]
E – Young's modulus, [Mpa]
H_f – heat factor, [–]
h – convection heat transfer coefficient, [Wm^{-2}K^{-1}]
J_2, J_1, J_o – Bessel functions, [–]
k – thermal conductivity, [Wm^{-1}K^{-1}]
l – laser rod length, [m]
N – number of total pulses, [–]
n – number of current pulse, [–]
P_{ab} – absorbed power, [W]
q – heat generation, [Wm^{-3}]
r – radial co-ordinate, [m]
T – temperature, [°K or °C]
T_o – period, [s]
t – time, [s]
t_o – pulse width, [s]
z – axial co-ordinate, [m]

Greek symbols

α – absorption coefficient, [cm^{-1}]
γ – coefficient of thermal expansion [K^{-1}]
ρ – density, [kgm^{-3}]
σ – stress, [MPa]
τ – pumping time, [s]
υ – Poisson's ratio, [–]

Subscripts

a – air
e – edge
o – outside
1 – pumping
rr – radial
zz – axial
$\theta\theta$ – radial
∞ – enviernmental

References

[1] Bernhardi, E. H., Modeling Diode-Pumped Solid-State Lasers, Msc thesis, School of Physics, University of Kwazulu-Natal, Durban, South Africa, 2008
[2] Clarkson, W. A , Thermal Effects and their Mitigation in End-Pumped Solid-State Lasers, *J. Phys. D: Appl. Phys., 34* (2001), 16, pp. 2381-2395
[3] Pfistner, C., *et al*., Thermal Beam Distortions in End-Pumped Nd:YAG, Nd:GSGG and Nd:YLF, *IEEE J. Quantum Electron*., *30* (1994), 7, pp. 1605-1615
[4] Robinson, A. M., Thermal Transient Effects in Optically Pumped Repetitively Pulsed Lasers, *IEEE Journal of Quantum Electronics*, *7* (1994), 5, pp. 1605-1615
[5] Huang, F., *et al.*, Modeling and Resolving Calculation of Thermal Effect in Face-Pumped High Power Heat Capacity Disk Laser, *Proceedings*, SPIE 6823, High-Power Lasers and Applications IV, Beijing, China, 2008, Vol. 6823, pp. 682311-628319
[6] Bernhardi, E. H., *et al.*, Estimation of Thermal Fracture Limits in Quasi-Continuous-Wave End-Pumped Lasers through a Time-Dependent Analytical Model, *Optics Express*, *16* 2008), 15, pp. 11115-11123
[7] Liu, T., *et al.*, Analytical Investigation on Transient Thermal Effects in Pulse End-Pumped Short-Length Fiber Laser, *Optics Express*, *17* (2009), 15, pp. 12875-12890
[8] Shibib, K. S., *et al*., Analytical Model of Transient Thermal Effect on Convectional Cooled End-Pumped Laser Rod, *Pramana-Journal of Physics, Indian Academy of Sciences*, *81* (2013), 4, pp. 603-615
[9] Shibib, K. S., *et al*., Analytical Treatment of Transient Temperatureand Thermal Stress Distribution in CW End Pumped Laser Rod: Thermal Response Optimization Study, *Thermal Science*, *18* (2014), 2, pp. 399-408
[10] Bergman, T. L., *et al*., *Fundamentals of Heat and Mass Transfer*, 7th ed., John Wiley & Sons, London, 2011
[11] Holman, J. P., *Heat Transfer*, 10th ed., McGraw-Hill, New York, USA, 2010
[12] Cousins, A. K., Temperature and Thermal Stress Scaling in Finite-Length End-Pumped Laser Rods, *IEEE Journal of Quantum Electronics*, *28* (1992), 4, pp. 1057-1069
[13] Ozisik, M. N., *Heat Conduction*, John Wiley and Sons, New York, USA, 1980
[14] Frauchiger, J., *et al*., Modeling of Thermal Lensing and Higher Order Ring Mode Oscillation in End-Pumped CW Nd:YAG Lasers, *IEEE J. Quantum Electron*, *28* (1991), 4, pp. 1046-1056
[15] Xiuer, P., *Thermal Stress and Thermal Fatigue*, National Defense Industry Press, Beijing, 1984
[16] Shibib, K. S., *et al*., Analytical Model of Transient Temperature and Thermal Stress in Continuous Wave Double-End-Pumped Laser Rod: Thermal Stress Minimization Study, *Paramana Journal of Physics*, *79* (2012), 2, pp. 287-297

Paper submitted: October 11, 2014
Paper revised: March 20, 2015
Paper accepted: March 29, 2015
© 2017 Society of Thermal Engineers of Serbia
Published by the Vinča Institute of Nuclear Sciences, Belgrade, Serbia.
This is an open access article distributed under the CC BY-NC-ND 4.0 terms and conditions